Automatic Biomechanical Workload Estimation for Construction Workers by Computer Vision and Smart Insoles

Yu, Yantao; Li, Heng; Umer, Waleed; Dong, Chao; Yang, Xincong; Skitmore, Martin; Wong, Arnold Y.L.

Published in:
Journal of Computing in Civil Engineering

DOI:
10.1061/(ASCE)CP.1943-5487.0000827

CP2800

Automatic Biomechanical Workload Estimation for Construction Workers by Computer Vision and Smart Insoles

Yantao Yu,[1] Heng Li,[2] Waleed Umer,[3] Chao Dong,[4] Xincong Yang,[5] Martin Skitmore,[6] and Arnold Y. L. Wong[7]

[1] Ph.D. Student, Department of Building and Real Estate, Hong Kong Polytechnic University, Rm ZN1002, Hung Hom, Kowloon, Hong Kong SAR. Email: yt.yu@connect.polyu.hk
[2] Chair Professor, Department of Building and Real Estate, Hong Kong Polytechnic University, Rm ZS734, Hung Hom, Kowloon, Hong Kong SAR. Email: heng.li@polyu.edu.hk
[3] Research Associate, Department of Building and Real Estate, Hong Kong Polytechnic University, Rm ZN1002, Hung Hom, Kowloon, Hong Kong SAR. Email: waleed.umer@connect.polyu.hk
[4] Ph.D. Candidate, School of Civil Engineering and Mechanics, Huazhong University of Science and Technology, Luoyu Road 1037, Hongshan District, Wuhan, China. Email: daisydc@hust.edu.cn
[5] Ph.D. Candidate, Department of Building and Real Estate, Hong Kong Polytechnic University, Rm ZN1002, Hung Hom, Kowloon, Hong Kong SAR (corresponding author). Email: xincong.yang@outlook.com
[6] Professor of Construction Economics and Management, Room S711, School of Civil Engineering and Built Environment, Queensland Univ. of Technology, Gardens Point, Brisbane Q4001, Australia; Visiting Professor, Faculty of Computing, Engineering and the Built Environment, Birmingham City Univ., Birmingham B4 7BD, UK; Guest Professor, Research Institute of Complex Engineering and Management, School of Economics and Management, Tongji Univ., Shanghai 200092, China; International Collaborative Partner, Universiti Tunku Abdul Rahman Global Research Network, Kuala Lumpur, Malaysia. Email: rm.skitmore@qut.edu.au
[7] Assistant Professor, Department of Rehabilitation Sciences, Hong Kong Polytechnic University, Room No. ST512, Hung Hom, Kowloon, Hong Kong SAR. Email: arnold.wong@polyu.edu.hk

Abstract

Construction workers are commonly subject to ergonomic risks due to awkward working postures or lifting/carrying heavy objects. Accordingly, accurate ergonomic assessment is needed to help improve efficiency and reduce risks. However, the diverse and dynamic nature of construction activities makes it difficult to unobtrusively collect worker behavior data for analysis. To address this issue, an automatic workload approach is proposed for the first time to continuously assess worker body joints using image-based 3D posture capture smart insoles, and biomechanical

analysis to provide detailed and accurate assessments based on real data instead of simulation. This approach was tested in an experiment, indicating that the method was able to automatically collect data concerning the workers' 3D posture, estimate external loads, and provide the estimated loads on key body joints with an error rate of 15%. In addition to helping prevent construction workers' ergonomic risks, the method provides a new data collection approach that may benefit various behavior research fields related to construction safety and productivity management.

Keywords: construction, worker, workload, occupational health and safety, ergonomic risks, biomechanical analysis, automated image-based 3D posture estimation, smart insoles, machine learning, deep learning.

Introduction

Workplace health and safety is an important issue worldwide. This is particularly the case with construction workers because of the heavy physical workload involved in their tasks (Inyang et al., 2012; Umer et al., 2018). Construction activities often demand repetitive, awkward, postures and overexertion from the workers; the amount of work required and tight time schedules involved making them busy for prolonged durations with minimal breaks. Such a physical workload increases the likelihood of fatigue - the most frequent reason for accidents in the oil and gas industry, for instance (Chan, 2011), and an important root cause of accidents in the construction industry too. Workers continuing to work under fatiguing conditions face high health risks because of the development of work-related musculoskeletal disorders (MSDs). According to the U.S. Bureau of Labor Statistics (2016), 33% of all occupational injuries and illnesses on U.S. construction sites are related to fatigue and overexertion. Fatigue and MSD can also decrease construction worker productivity (Aryal et al., 2017).

A first step towards lessening their negative influence is to precisely assess the workloads involved. Manual observation is frequently used for this, based on workers' postures and external loads - the observation results are usually quantitatively analyzed with ergonomic scales. However, this method is too subjective to provide sufficiently accurate assessments. To address this limitation, a previous study has used biomechanical measurement devices to analyze workload (Umer et al., 2017b). Despite proving the concept, these approaches require the attachment of multiple sensors to the worker's body, which may cause physical discomfort and irritation, as well as adversely affect productivity.

Considering the limitations of these methods, we propose a blend of computer vision technology and smart insoles for the workload assessment and visualization of construction workers by providing a novel non-intrusive means to monitor whole-body workload. First, smart insoles equipped with 26 pressure sensors are used to capture workers' plantar pressure. These pressure sensors register the force due to the workers' self-weight and other external forces while carrying loads, operating tools, etc. Second, an RGB (red-green-blue) camera computer is used in conjunction with a specially developed vision-based motion capture algorithm to model the motions of a worker's various body parts while performing construction tasks. Inverse dynamics, applied to the 3D posture data from the motion capture algorithm and force data from the insoles, is used to calculate the joint torque, which is then compared with individual joint capacity to estimate the workload borne by each joint.

The proposed approach is both practically and theoretically significant. The development of such a system would equip the industry with a non-invasive tool for workload monitoring. Specifically, the visualized results will help construction workers and managers have an intuitive understanding of whole-body workloads and ergonomic risks. The posture and external load data also contain rich information of work patterns and workloads that could help understand the

relationship between construction activities and workloads, provide a data base for refining ergonomic guidelines (e.g., work-rest schedule and work platform design), and improve the occupational health and safety of the industry.

The remainder of this paper is arranged as follows. First, a literature review summarizes relevant workload assessment methods and identifies the gap between existing methods and the demands of construction applications. Second, a research framework is introduced, and the method is then demonstrated to test the feasibility and accuracy of the approach. Finally, the method's advantages and shortcomings are summarized in the discussion and conclusion, where some suggestions are provided for further improvement.

Literature review

The purpose of this review is to provide an understanding of the previous research in this area as well as providing a rationale for the choice of workload assessment and data collection methods used in the present study. We begin with a review of the definitions and influences of workloads; two workload assessment methods, scales and biomechanical analysis, are then reviewed and compared; this is followed by a discussion of the behavior data collection methods used previously in the construction context.

Definition of physical workload

Workload represents all the factors reflecting the amount of difficulty of a person's work, including physical workload and mental workload (Bowling and Kirkendall, 2012). This research focuses on physical workload because this has been proved to be a major factor leading to acute trauma injuries and cumulative MSDs (Radwin et al., 2001; Van Nieuwenhuyse, 2006), and it is more practical to provide a relatively objective and quantitative assessment of physical workload with

current technical support. Physical workloads have two different definitions according to different load measurements, i.e. biomechanical load and cardiovascular load (Sandmark et al., 1999). Biomechanical load measures workload as the force or torque acting on the human body, which can be estimated by observation or computer vision, while cardiovascular load measures workload with cardiovascular indicators. The measurement of cardiovascular indicators usually involved wearable sensors with direct skin contact, which might be uncomfortable and irritating to wear (Sandmark et al., 1999). Moreover, biomechanical load has a more intuitive and direct relationship with external load and work duration. In short, workload assessment from a biomechanics perspective can provide direct suggestions for ergonomic improvements (Winkel and Mathiassen, 1994). Based on these considerations, therefore, the present research assesses physical workload from the biomechanical perspective. The term *"physical workload"* is used to represent *"physical workload from biomechanical perspective"* for the remainder of the paper.

Physical workload is the physical stress acting on a body, where stress is determined by working posture, the magnitude and location of external forces (such as hand loads and ground reaction forces), and the repetition and duration of working posture or external forces. The methods that have been proposed to measure physical workload from these aspects are reviewed in the following section.

Workload assessment methods

Scales for workload assessment.

Ergonomic scales assess the level of workload according to work posture, external load, repetitiveness, and duration. A variety of scales have been developed and applied, e.g. OCRA (Occupational Repetitive Actions) (Occhipiniti, 1998), RULA (Rapid Upper Limb Assessment) (McAtamney and Nigel Corlett, 1993), and REBA (Rapid Entire Body Assessment (Hignett and

McAtamney, 2000). These tools are easy to use and provide quantitative workload assessments. However, most methods focus on only a few aspects of the workload factors involved. For example, RULA and REBA just assess whole body workload, while OCRA focuses on the upper body only; REBA and RULA consider static load, while OCRA considers workload repetitiveness and duration. Most scales define body posture quantitatively by the angle of the joints involved, but differ in their range of values. Consequently, assessing the same workload with different scales may lead to different results (Roman-Liu, 2014). In addition, these tools are aimed at manufacturing workers and consider motion and external load as repetitiveness, while the motion and external load patterns of construction workers are less regular, which make the scales difficult to apply in the construction situation. To solve these issues, we aim to develop a workload assessment method that is suitable for the complex nature of construction activities by using biomechanical analysis. The following section reviews the biomechanical-based workload assessment methods available.

Biomechanical analysis for workload assessment.

Biomechanical analysis measures physical workloads in terms of joint force or torque. The biomechanical approach simplifies the human body as a lever system and uses mechanics to calculate internal torques based on joint position, external loads, and the person's anthropometry parameters (Winkel and Mathiassen, 1994). Biomechanical analysis has been used to provide workload assessment in various contexts. Otsuka et al. (2010), for example, apply biomechanical methods to explore the relationship between work posture and workload during the insertion of pin connectors; Neumann et al. (2001) apply biomechanical analysis to assess low back pain risks; while the biomechanical method has also been successfully applied in the construction industry to facilitate the simulation of work-rest schedules (Seo et al., 2016a).

Theoretically, biomechanics involves all the key factors of workload assessment (the magnitude, repetitiveness, and duration of external forces and location). Without restrictions on motion or load pattern (i.e. repetitive motion and static external loads), biomechanical analysis can be applied to almost any work tasks and all parts of the body (Roman-Liu, 2014). The gap between theoretical analysis and real practice is the method of collecting the motion and external load data. Observation has been widely used to collect motion data in previous workload assessment studies (Neumann et al., 2001; Otsuka et al., 2010). However, the observed results are considered too subjective and inaccurate to support biomechanical analysis. It is also difficult to identify motion or load patterns based solely on manual observation (Valero et al., 2016). To solve these problems, several data collection methods have been applied to collect accurate workload-related data automatically; the following section reviews these methods.

Automatic data collection methods for workload assessment

Automatic posture data collection.

One widely used sensor system for capturing motion is the inertial measurement unit (IMU). If attached to key joints, IMU sensors are able to capture the accurate location and acceleration of the joints automatically (Yan et al., 2017). Previous research has used IMU to successfully collect posture data for workload assessment (Nath et al., 2017). The main disadvantage, however, is the necessary to tie IMU sensors tightly to the human body – an intrusiveness that may not be acceptable in practice. As Golabchi et al. (2016) and Valero et al. (2016) comment, such sensors may be feasible for a short-period but are likely to be irritating in long-time applications.

The development of computer vision has prompted the proposal of various video-based methods to collect worker posture data, as cameras are clearly less intrusive than body sensors. Depth cameras have been particularly successful in workload evaluation (Ning and Guo, 2013),

and several studies have applied them in construction management to recognize worker actions, (Ray and Teizer, 2012), for example, or to capture worker joint angles (Yu et al., 2017). However, although depth cameras have proven to be an efficient tool for collecting posture data for ergonomic evaluation in laboratory conditions, their inability to work under direct sunlight limits their application on construction sites

Other research has extracted posture information based on RGB pictures from ordinary cameras. Shin et al. (2014), for example, have successfully classified workers' postures with a double-lens camera; Seo et al. (2016b) propose a computer vision-based framework to identify construction activities from 2D image sequences; while Seo et al. (2016b) and Yan et al. (2017) use cameras to capture worker posture. However, while these methods are suitable for outdoor environments and can provide the non-intrusive workload estimation needed, they cannot support the 3D biomechanical analysis needed for construction workload assessment.

Recent progress in computer vision is now making 3D biomechanics-based workload assessment possible, however. This involves a newly-developed computer vision algorithm that can model a 3D human skeleton from 2D video frames, making it possible to collect 3D joint positions based solely on videos or images (Zhou et al., 2017). Here, we examine the algorithm's potential as a novel method for collecting construction worker behavior data and test its accuracy with construction activities experimentally.

Automatic external load data collection.

The use of insole-shaped plantar pressure sensors in the workers' footwear provides a potentially very efficient means of collecting external load data automatically. Two such sensor can collect the total ground reaction force of both feet (Lin Shu et al., 2010) then, by comparing this with the worker's self-weight, the external loads involved can thus be estimated. This sensor has been

widely used in biomedicine to collect plantar pressure data (Zeng et al., 2014). Importantly for the construction context, it is also is portable and non-intrusive. Recently, Antwi-Afari et al. (2018) have demonstrated the potential of applying the smart insole to obtain the plantar pressure of construction workers without interfering with their normal construction activities. Here, we obtain the external loads involved by applying the smart insoles continuously to obtain the ground reaction force involved.

In summary, the prospects of automatic construction industry workload assessments are limited in that they: 1) lack a workload assessment method suited to the complex posture and load patterns of construction activities; and 2) lack a behavior data collection method (including posture data and external load data) for construction workers that is automatic, accurate, and non-intrusive. Here, we solve these problems by automatic biomechanical analysis, involving a new workload assessment method based on a posture model from computer vision data provided by algorithms, and external load data provided by smart insoles. The method could provide a relatively accurate and objective workload assessment for construction workers, which could not only offer the workers an improved understanding of the ergonomic risks involved, but also provide the data foundation for further studies of construction worker health, safety, and productivity.

Method

Outline

Figure 1 depicts the flowchart of the proposed construction worker's workload evaluation method. The input data includes video frames or pictures recorded with cameras, plantar pressure data collected with pressure sensors, and anthropology parameters of age, gender, height, and weight. The data processing period contains five tasks: 1) estimating 3D joint coordinates with a deep learning algorithm; 2) estimating external loads according to the plantar pressure data; 3)

estimating joint capacity based on anthropology parameters; 4) calculating joint torque according to the 3D joint coordinates and external loads; and 5) assessing workload based on joint torque and joint capacity.

3D posture capture from 2D images

To ensure the non-intrusiveness of behavior data collection, the posture data must be collected automatically without interfering with work activities. This involves the use of computer vision. The workflow of the 3D pose estimator is shown in Figure 2 and comprises two steps of 2D joint recognition and 3D joint coordinate estimation.

2D joint recognition.

The aim of 2D joint recognition is to recognize the key joints and estimate their 2D coordinates. For this, a hourglass network is applied (Newell et al., 2016), which is a deep learning network that describes the relationship between pixels or pixel groups with multi-layer neuron networks. The hourglass network considers the features of both the local area and the whole image, making it suitable for joint recognition, which requires the recognition of each joint and the entire human body. A MPII (Max Planck Institute for Informatics) Human Pose dataset, which contains 25,000 pictures of various activities and the 2D coordinates of each joint, is used to train the hourglass network (Andriluka et al., 2014). Given the picture as input and 2D joint coordinates as output, the network is trained to find the best weight of each neuron so it can minimize the error between estimated joint coordinates and the real coordinates. The result of this step is a series of possibility distribution maps of the recognized joints, as shown in Figure 2.

Estimation of the 3D joint coordinates.

The aim of this step is to infer the 3D joint coordinates based on the 2D joint coordinates. It is usually difficult to infer 3D information solely from 2D information. However, the human body has bone length constraints, which links the 3D joint coordinates with 2D joint coordinates. Another deep learning algorithm is applied to simulate the complex nonlinear relationship between the 3D and 2D joint coordinates (Zhou et al., 2017). The algorithm is trained on a Human 3.6M dataset (which includes the 2D and 3D coordinates of 3.6 million postures) to minimize the differences between the estimated and actual 3D coordinates. An example of a 3D joint location estimate is given in Figure 2.

Automatic external load measurement

The novel insole with plantar pressure sensors, named *Moticon*, is used to measure the worker's total weight, including self-weight and other forces, as shown in Figure 3. The insole can be used in virtually any footwear. These commercial available smart insoles can transfer data wirelessly through an ANT radio service (Stöggl and Martiner, 2017).

Each pair of insoles contains 26 pressure sensors (13 in each insole) as shown in Figure 4 to measure the corresponding area's average pressure. The total ground reaction force of the insole equals the pressure of each sensor multiplied by the sensor area, with

$$\begin{bmatrix} F_L \\ F_R \end{bmatrix} = \frac{S}{N+1} \sum_{n=0}^{N} \begin{bmatrix} p_{L,n} \\ p_{R,n} \end{bmatrix} \quad (1)$$

where F_L, F_R [N] is the ground reaction force of the left foot (L) and right foot (R); S is the plantar contact area of each foot (S =150 cm^2); N is the largest sensor number (#), (N =12; N+1=13 is the total number of sensors in each insole); $n \in \{n \in \mathbb{R} \mid 0 \leq n \leq N\}$ is the number (#) of each sensor, $p_{L,n}$, $p_{R,n}$is the pressure value measured by sensor n in the left (L) or right insole (R).

It should be noted that the insole-based weight and external burden estimation method involves the following assumptions:

a) All the worker's weight and external load act on his/her feet, which means that this method is unsuitable for such postures as leaning against a wall or sitting on the floor;
b) The worker's posture has no acceleration in the vertical direction. Otherwise, the ground reaction force measured with the insoles does not equal to the weight of worker and any external burden.

The amount of external load is the total weight minus the worker's self-weight. In construction tasks, external loads are usually located at the hands and feet (the ground reaction force). For the force located at the hands, two-arm and one-arm working patterns are taken into consideration. The angles of the shoulder joints and elbow joints on both sides are compared to identify the pattern. If the angles of the left and right arm are the same, the working pattern is considered a two-arm working pattern. Otherwise, a one-arm working pattern is identified, and the external load is considered at the worker's dominant hand.

Workload assessment based on biomechanical analysis

Workload assessment aims to calculate the joint torques, and assess workload based on these and the workers' joint capability.

Calculation of joint torques.

Given the workers' posture (3D coordinates of key joints) and external loads, biomechanical analysis is used to calculate the torque of each joint based on Newton's Laws of Motions. To facilitate biomechanical analysis, the human body skeleton is simplified as a lever-hinge system, in which levers represent bones and hinges represent joints. An assumption is made that the motion

of the workers' key joints is steady and slow, which means the joints are in equilibrium. Figure 5 illustrates the biomechanical simplification of the analysis of a forearm. In the elbow torque calculation, the forearm is simplified as a lever, where points A, B, and C represent the elbow's location, the forearm's gravity center, and location of the hand. The location of point C (i.e. the gravity center of a certain body segmentation) is given in Standardization Administration of China (1988, 2004). Since the forearm is assumed to be in equilibrium, the respondent torque at the elbow can be obtained. The external load in Figure 5 includes the self-weight of the forearm and the two bricks.

The elbow torque is given by

$$T = W_{forearm} \times A_{cl} + W_{brick} \times A_{cr} \qquad (2)$$

$$A_{cl} = L_{cl} \times cos\,\theta\,, A_{cr} = L_{cr} \times cos\,\theta$$

$$\theta = arctan \frac{|y_A - y_B|}{\sqrt{(x_A - x_B)^2 + (z_A - z_B)^2}}$$

where T is the elbow torque; W_{forearm}, W_{brick} are the forearm and brick weights; A_{cl}, A_{cr} are the force arms of W_{forearm}, W_{brick}; L_{cl} and L_{cr} are the lengths of the two parts of the forearm divided by its gravity center (point C); θ is the angle between the forearm and the horizontal plane;

The coordinates of points A and B are $A(x_A, y_A, z_A)$ and $B(x_B, y_B, z_B)$.

Automatic biomechanical analysis software 3DSSPP is used to calculate the joint torques, as this is a relatively complex operation.

Joint workload assessment.

Given the joint torque, this section aims to provide a workload assessment based on the workers' load tolerance. The basic assumption is that different people have a different load tolerance, so workload assessment should consider not only such external factors as external loads and postures,

but also the workers' capability to tolerate loads. Maximal isometric strength (MVIC) is a widely used indicator to measure the human body's biomechanical capacity. Consortium (1996) has developed a regression equation to predict MVIC based on gender, age, height, and weight, from the results of more than 500 experiments. This is used to estimate joint capability, with

$$T_{max} = \left(-a \times age + b \times gender + c \times \frac{weight}{height^2} + d) \times l_{bone}\right) \qquad (3)$$

where T_{max} represents the maximum torque the joint can tolerate (the unit is [N]); l_{bone} is the force arm length during measuring external loads (the unit is [m]) - as the joint angles in the experiment are right angles, the force arm is equal to the corresponding bone's length; gender =1 if the subject is a male; gender =0 if female; The units of age, weight, and height are [year], [kg], and [m] respectively; a, b, c and d are the coefficients, whose value is given in Table 1.

Based on the current joint load T [N] and joint load capability T_{max} [N], the joint workload is then given by

$$Workload = \frac{T}{T_{max}} \times 100\% \qquad (4)$$

Experiments, results and analysis

Experimental design

Three main construction activities involved in the experiment are shown in Figure 6; these comprise material handling, rebar, and plastering. Three people participated in the experiment. Each wore smart insoles to capture the self-weight and any external load. A smart phone camera fixed on a tripod recorded the whole process. At the same time, a set of IMU sensors tied to the subject's main joints also recorded the location of the joints. The IMU sensor has an accuracy of

up to 1 degree (Yost Labs, 2017). Experiments were enacted in both indoor and outdoor environments to demonstrate the feasibility of the proposed method.

Experiment data

The video data frequency is 25 fps (frames per second), and the insole pressure data is 50 fps. The 3D joint coordinates, ground reaction forces, and hand loads were calculated and synchronized based on the method described. Table 2 provides the raw data.

Posture data.

The 3D joint locations were extracted from the video frames by the 3D pose estimator. Figure 7 shows one frame of the captured data. The 3D joint location data of each frame is a 16×3 matrix composed of the 3D coordinates of 16 joints. The IMU data was used to validate the 3D posture estimation algorithm's accuracy, with video clips being first separated to more than 3,000 frames, and then the 3D pose estimator applied to each frame to obtain the 3D coordinates of each joint. The joint angles measured with the IMU sensors were transferred the joint locations and the two joint location estimation results compared. The results indicate the accuracy of the computer vision- based 3D posture estimation method to be approximately 3 cm per joint (Figure 8).

Plantar pressure data.

Pressure data was used to evaluate the worker's self-weight and other forces. In the material handling experiment, the subjects were required to lift various numbers (0~4) of bricks and hold them for 10 seconds. Each brick weighs 2 kg (19.6 N (g= 9.8 m/s^2)). Figure 9 shows the postures involved in holding the bricks.

At the same time, the total weight, i.e. the ground reaction force, was measured by the smart insoles. Each sensor recorded the corresponding area's average pressure data (shown in Figure 5). Figure 10 presents an example of the pressure data recorded by the No. 8 sensor in the right insole when the subject was carrying 3 bricks. The pressure data was estimated as 2.5 N/cm^2. Table 3 provides the pressure values of all the 13 pressure sensors in the right insole.

Figure 11 shows the ground reaction forces of both feet and the total ground reaction forces when the subject is holding 0~4 bricks. The brick weight was calculated as the difference between the ground reaction forces of consecutive liftings, as shown in Figure 12. The real weight of each brick is 19.6 N. The relative error is 5.99%, given by

$$\delta = \frac{1}{N}\sum_{i=1}^{N}\frac{|w_i - w|}{w} \times 100\% \quad (5)$$

Where δ is the relative error; N is the total number of trials (N=4); i is the brick number (i ∈ {1,2,3,4}); w_i is the estimated weight of the i^{th} brick; w is the brick's real weight.

Based on this analysis, the subject's self-weight was measured as 725.8N, and weights of the four bricks were 17.5N, 20.2N, 18.2N, and 19.0N.

Joint torque results.

Given the above position and external data, the joint torques were calculated with the 3DSSPP biomechanical analysis module. Table 4 contains part of the joint torque results in the material handling experiment.

Workload assessment results.

Based on the joint torque and joint capability data (Table 4), the workload of each joint was assessed as the percentage of the joint torque in joint capacity (Table 5).

Figure 13 shows the joint workload distributions during typical postures of the three construction activities involved. These comprise: 1) material handling: standing, bending when lifting the brick(s), standing again with the brick(s); 2) plastering: moving the arm from right to left; and 3) standing, bending, and rebar. The joint workloads in the skeleton figures are presented in Figure 14.

The error of joint torque was analyzed according to joint location and external load errors. As the forearm is the nearest joint with the external load in the experiment, and the self-weight of forearm is smaller than other body segments, the elbow torque was selected to calculate the maximum error of joint torque. Considering the forearm model in Figure 5, this can be calculated from

$$T = \alpha l W_{forearm} + l W_{brick} = l(\alpha W_{forearm} + W_{brick})$$

$$T + \Delta T = (l + \Delta l)(\alpha W_{forearm} + W_{brick} + \Delta W_{brick})$$

$$\frac{\Delta T}{T} = \frac{\Delta l}{l} + \frac{\Delta W_{brick}/W_{brick}}{\alpha W_{forearm}/W_{brick} + 1} + \frac{\Delta l}{l} \times \frac{\Delta W_{brick}/W_{brick}}{\alpha W_{forearm}/W_{brick} + 1} \quad (6)$$

$$\cong \frac{\Delta l}{l} + \frac{\Delta W_{brick}/W_{brick}}{\alpha W_{forearm}/W_{brick} + 1}$$

Where α is the ratio of the force arm of $W_{forearm}$ and the force arm of W_{brick}; l is the force arm of W_{brick}; Δl , ΔW_{brick} and ΔT represent the errors of l , W_{brick} and T respectively .

According to the joint coordinate and external load errors, $\Delta W_{brick}/W_{brick}$= 5.99% and Δl =3 cm. Assume l= 30 cm and $\alpha W_{forearm}$= 0.4 kg, then the elbow torque error was approximately 15%. The whole physical workload assessment progress (from identifying 3D joint coordinates to visualizing the joint workload with the 3D skeleton) took around 0.5s in one GTX 1080Ti on a

Linux PC with Ubuntu 16.04 system and MATLAB (2014a) on a WINDOWS 10 PC (Intel Core i7-5500U @ 2.4GHz, 8.00GB RAM).

The workload assessment results demonstrated that the proposed methodology could automatically provide joint-level workload assessment for construction workers. The results also provide actual data-based workload assessment and suggestions. Comparing the joint workload of three construction activities indicates that material handling is more likely to result in high joint workload than plastering and rebar. In all the three activities, the left hip and left knee had a higher workload than other joints in the experiments, suggesting that the subjects may need to reduce the left leg workload by balancing the workload of both legs. Figure 14 provides more detailed and intuitive information concerning material handling. In the experiment, two subjects were required to lift four bricks by bending lifting and squatting lifting. It can be observed that the workloads of the squatting lifting were smaller, confirming the well-known fact that squatting lifting is a better posture for material handling.

Field test of the proposed methodology

To test the feasibility of the proposed methodology on construction site, two experiments were conducted. The first experiment tested the feasibility of the 3D posture capture method on construction sites. Three construction workers (a rebar worker, a masonry worker and a paving worker in the first experiment) participated the experiment for around 10 minutes. During the experiment, the rebar worker was tying the rebars in the squatting posture; the masonry worker was mixing mortar batches; and the paving worker was leveling the ground. Figure 15 illustrates several representative frames of a rebar worker, a masonry worker and a concreter in the first experiment. It was found that the three workers could be successfully identified. However, in the rebar worker experiment, the first two frames had significant errors, indicating that the method

could not infer the joint locations accurately during tasks with severe visual obstacles, i.e., the right side of the workers body was blocked by the left side of the body. The experiment of the masonry worker demonstrated that the 3D motion capture method could work under poor lighting conditions. The experiment of the concrete worker demonstrated the suitability to outdoor environments under direct sunlight.

The second experiment tested the feasibility of the workload assessment method. In particular, a masonry worker was instructed to build a concrete block wall as shown in Figure 16. Figure 17 shows several frames of the experiment frames. Figure 18 and Figure 19 show the joint-level workload results of a masonry worker. The eight curves in Figure 18 represent the workload of the eight joints (left/right shoulder/elbow/knee/ankle) in each frame, which demonstrates the fierce fluctuation of the joint workloads over time. Figure 19 presents each joint-level workloads graphically, where the blue bars represent the average joint workloads of the eight target muscles during the masonry task, and the green lines are the minimum and maximum workloads of each joint. It reveals that the left shoulder and right elbow have the highest workload average and the highest workload maximum.

Discussion

This study proposes a workload assessment method aiming to solve the on-site workload assessment problem automatically, non-intrusively, and reasonably accurately with deep learning posture estimation algorithms, pressure sensors, and biomechanical analysis. A novel computer vision algorithm is used that can estimate 3D joint coordinates from 2D images. According to the experimental results, the estimation error is around 3 cm per joint. While this is higher than that of the depth camera (Kinect, 2 cm per joint) and motion sensor (YEI3, 1 degree) (Khoshelham and Elberink, 2012; Yost Labs, 2017), the method is non-intrusive and is suited to both indoor and

outdoor environments. An additional benefit is that the pose estimation method can also be used in other posture-related research, such as construction worker safety and productivity management.

Another contribution of the research is the automatic external load data collection. External load is a key factor in workload assessment and has been involved in several classical workload assessment methods (Golabchi et al., 2015). However, this is the first method for collecting external load data automatically and, with an experimental material handing error rate of approximately 6%, makes the subsequent automatic biomechanical analysis entirely feasible.

The percentage of joint torque in joint capacity used as the workload indicator is also reasonably accurate, with an experimental error rate of approximately 15%. Its advantage in comparison with traditional ergonomic scales is that it is not limited to work posture, duration, and repetitiveness, and thus is more suitable for the complex and dynamic nature of construction activities. In addition, the method can also individualize workload assessment by considering joint capacity. The joint-level workload assessment provides a construction site database for such ergonomic improvements as suggested by the actual work postures being exhibited.

A limitation of the method is the assumption that motions are relatively slow and steady, and therefore we simply use statistics when calculating the joint torques; when the workers' motion is not steady, however, the acceleration will increase the joint torque. Further, when estimating external loads, it was assumed that all worker pressure was on the feet. Although this assumption may be true for most construction works, it is not applicable for situations where workers are sitting or sharing their body weight on their knees. The method assumes the joint capacity to be a constant throughout the experiment - while it is possible that continuous working could lead to a decrease in joint capacity, and thus an increase in the ratio of joint torque to joint capacity. In addition, the field test showed that when a worker was squatting, the 3D motion capture method

couldn't correctly identify the joints. This implies that this method may not be accurate if the vision is blocked.

As well as examining the implications of these limitations, further research could consider improving the method's accuracy using dynamics to analyze the joint torques if the acceleration data can be collected; developing more accurate external load estimation methods, such as by first identifying the carried object with deep learning algorithms and using the information to help estimate its weight; and estimating joint capacity more accurately by considering not only the workers anthropology parameters but also external load and work duration data. To improve the 3D motion algorithm accuracy, the 3D motion estimation algorithm should be trained with more construction site pictures, especially those with higher visual obstacles between the worker and the camera.

Conclusion

A novel automatic workload assessment approach is presented by merging computer vision, pressure sensor technology, and biomechanical analysis. The method collects worker posture data with computer-vision algorithms and smart sensor insoles, which makes it possible to collect behavioral data non-intrusively and accurately. With a response time of approximately half a second and an experimental error of 3 cm per joint for joint position, 5.99% for workload, and 15% for body joint load estimation, the method is demonstrated as being capable of successfully estimating joint-level workload based on video records and plantar sensors. The method potentially contributes to the collection of behavior data and ergonomic improvements of construction workers. Moreover, the workload assessment is based on biomechanical assessment, which is eminently suited to the complex and diversified nature of construction activities.

References

Abdelhamid, T. S., & Everett, J. G. (2000). Identifying root causes of construction accidents. *Journal of Construction Engineering and Management*, *126*(1), 52-60. https://doi.org/10.1061/(ASCE)0733-9364(2000)126:1(52)

Andriluka, M., Pishchulin, L., Gehler, P., & Schiele, B. (2014). 2D human pose estimation: New benchmark and state of the art analysis. In *Proceedings of the IEEE Computer Society Conference on Computer Vision and Pattern Recognition* (pp. 3686–3693). IEEE. https://doi.org/10.1109/CVPR.2014.471

Antwi-Afari, M. F., Li, H., Darko, A., Seo, J., Wong, A. Y., & Yu, Y. (2018). Automated Detection and Classification of Construction Workers' Awkward Working Postures using Wearable Insole Pressure Sensors. *1st Postgraduate Applied Research Conference in Africa*. Accra, Ghana. https://www.researchgate.net/publication/323689588_Automated_Detection_and_Classification_of_Construction_Workers'_Awkward_Working_Postures_using_Wearable_Insole_Pressure_Sensors

Aryal, A., Ghahramani, A., & Becerik-Gerber, B. (2017). Monitoring fatigue in construction workers using physiological measurements. *Automation in Construction*, *82*, 154–165. https://doi.org/10.1016/j.autcon.2017.03.003

Bowling, N. A., & Kirkendall, C. (2012). Workload: A Review of Causes, Consequences, and Potential Interventions. In *Contemporary Occupational Health Psychology* (Vol. 2, pp. 221–238). Chichester, UK: John Wiley & Sons, Ltd. https://doi.org/10.1002/9781119942849.ch13

Chan, M. (2011). Fatigue: The most critical accident risk in oil and gas construction. *Construction Management and Economics*, *29*(4), 341–353.

https://doi.org/10.1080/01446193.2010.545993

Consortium, N. I. M. S. D. (1996). Muscular weakness assessment: Use of normal isometric strength data. *Archives of Physical Medicine and Rehabilitation*, *77*(12), 1251–1255. https://doi.org/10.1016/S0003-9993(96)90188-4

Golabchi, A., Han, S., & Fayek, A. R. (2016). A fuzzy logic approach to posture-based ergonomic analysis for field observation and assessment of construction manual operations. *Canadian Journal of Civil Engineering*, *43*(4), 294–303. https://doi.org/10.1139/cjce-2015-0143

Golabchi, A., Han, S., Seo, J., Han, S., Lee, S., & Al-Hussein, M. (2015). An Automated Biomechanical Simulation Approach to Ergonomic Job Analysis for Workplace Design. *Journal of Construction Engineering and Management*, *141*(8), 04015020. https://doi.org/10.1061/(ASCE)CO.1943-7862.0000998

Hignett, S., & McAtamney, L. (2000). Rapid Entire Body Assessment (REBA). *Applied Ergonomics*, *31*(2), 201–205. https://doi.org/10.1016/S0003-6870(99)00039-3

Inyang, N., Al-Hussein, M., El-Rich, M., & Al-Jibouri, S. (2012). Ergonomic Analysis and the Need for Its Integration for Planning and Assessing Construction Tasks. *Journal of Construction Engineering and Management*, *138*(12), 1370–1376. https://doi.org/10.1061/(ASCE)CO.1943-7862.0000556

Khoshelham, K., & Elberink, S. O. (2012). Accuracy and Resolution of Kinect Depth Data for Indoor Mapping Applications. *Sensors*, *12*(2), 1437–1454. https://doi.org/10.3390/s120201437

Lin Shu, Tao Hua, Yangyong Wang, Qiao Li, Feng, D. D., & Xiaoming Tao. (2010). In-Shoe Plantar Pressure Measurement and Analysis System Based on Fabric Pressure Sensing Array. *IEEE Transactions on Information Technology in Biomedicine*, *14*(3), 767–775.

https://doi.org/10.1109/TITB.2009.2038904

McAtamney, L., & Nigel Corlett, E. (1993). RULA: a survey method for the investigation of work-related upper limb disorders. *Applied Ergonomics*, *24*(2), 91–99. https://doi.org/10.1016/0003-6870(93)90080-S

Nath, N. D., Akhavian, R., & Behzadan, A. H. (2017). Ergonomic analysis of construction worker's body postures using wearable mobile sensors. *Applied Ergonomics*, *62*, 107–117. https://doi.org/10.1016/j.apergo.2017.02.007

Neumann, W. P., Wells, R. P., Norman, R. W., Frank, J., Shannon, H., & Kerr, M. S. (2001). A posture and load sampling approach to determining low-back pain risk in occupational settings. *International Journal of Industrial Ergonomics*, *27*(2), 65–77. https://doi.org/10.1016/S0169-8141(00)00038-X

Newell, A., Yang, K., & Deng, J. (2016). Stacked Hourglass Networks for Human Pose Estimation. *European Conference on Computer Vision*, 483–499. arxiv.org/abs/1603.06937

Ning, X., & Guo, G. (2013). Assessing spinal loading using the kinect depth sensor: A feasibility study. *IEEE Sensors Journal*, *13*(4), 1139–1140. https://doi.org/10.1109/JSEN.2012.2230252

Occhipiniti, E. (1998). OCRA: a concise index for the assessment of exposure to repetitive movements of the upper limbs. *Ergonomics*, *41*(9), 1290–1311. https://doi.org/10.1080/001401398186315

Otsuka, M., Nishimura, T., Seo, A., & Doi, K. (2010). Relationship between Work Position and Physical Work Load during Insertion of Pin Connectors (Theory and Methodology). *Journal of Japan Industrial Management Association*, *61*(5), 275–283. https://ci.nii.ac.jp/naid/10027761503/en/

Radwin, R. G., Marras, W. S., & Lavender, S. A. (2001). Biomechanical aspects of work-related

musculoskeletal disorders. *Theoretical Issues in Ergonomics Science*, *2*(2), 153–217. https://doi.org/10.1080/14639220110102044

Ray, S. J., & Teizer, J. (2012). Real-time construction worker posture analysis for ergonomics training. *Advanced Engineering Informatics*, *26*(2), 439–455. https://doi.org/10.1016/j.aei.2012.02.011

Roman-Liu, D. (2014). Comparison of concepts in easy-to-use methods for MSD risk assessment. *Applied Ergonomics*, *45*(3), 420–427. https://doi.org/10.1016/j.apergo.2013.05.010

Sandmark, H., Wiktorin, C., Hogstedt, C., Klenell-Hatschek, E. K., & Vingård, E. (1999). Physical work load in physical education teachers. *Applied Ergonomics*, *30*(5), 435–442. https://doi.org/10.1016/S0003-6870(98)00048-9

Seo, J., Lee, S., & Seo, J. (2016a). Simulation-Based Assessment of Workers' Muscle Fatigue and Its Impact on Construction Operations. *Journal of Construction Engineering and Management*, *142*(11), 04016063. https://doi.org/10.1061/(ASCE)CO.1943-7862.0001182

Seo, J., Yin, K., & Lee, S. (2016b). Automated Postural Ergonomic Assessment Using a Computer Vision-Based Posture Classification. In *Construction Research Congress 2016* (pp. 809–818). Reston, VA: ASCE. https://doi.org/10.1061/9780784479827.082

Shin, M., Lee, H.-S., Park, M., Moon, M., & Han, S. (2014). A system dynamics approach for modeling construction workers' safety attitudes and behaviors. *Accident Analysis & Prevention*, *68*(0), 95–105. https://doi.org/10.1016/j.aap.2013.09.019

Standardization Administration of China. Human Dimensions of Chinese Adults, Pub. L. No. GB/T 10000-1988, Standardization Administration of China 20 (1988). http://www.gb688.cn. https://doi.org/ICS 13.180

Standardization Administration of China. Inertial parameters of adult human body, Pub. L. No.

GB/T 17245-2004, Standardization Administration of China 20 (2004). http://www.gb688.cn. https://doi.org/ICS 13.180

Stöggl, T., & Martiner, A. (2017). Validation of Moticon's OpenGo sensor insoles during gait, jumps, balance and cross-country skiing specific imitation movements. *Journal of Sports Sciences*, *35*(2), 196–206. https://doi.org/10.1080/02640414.2016.1161205

U.S. Bureau of Labor Statistics. (2016). Nonfatal Occupational Injuries and Illnesses Requiring Days Away from Work. Retrieved April 20, 2018, https://www.bls.gov/news.release/osh2.toc.htm

Umer, W., Antwi-Afari, M. F., Li, H., Szeto, G. P. Y., & Wong, A. Y. L. (2018). The prevalence of musculoskeletal symptoms in the construction industry: a systematic review and meta-analysis. *International Archives of Occupational and Environmental Health*, *91*(2), 125–144. https://doi.org/10.1007/s00420-017-1273-4

Umer, W., Li, H., Szeto, G. P. Y., & Wong, A. Y. L. (2017a). Identification of Biomechanical Risk Factors for the Development of Lower-Back Disorders during Manual Rebar Tying. *Journal of Construction Engineering and Management*, *143*(1), 04016080. https://doi.org/10.1061/(ASCE)CO.1943-7862.0001208

Umer, W., Li, H., Szeto, G. P. Y., & Wong, A. Y. L. (2017b). Low-Cost Ergonomic Intervention for Mitigating Physical and Subjective Discomfort during Manual Rebar Tying. *Journal of Construction Engineering and Management*, *143*(10), 04017075. https://doi.org/10.1061/(ASCE)CO.1943-7862.0001383

Valero, E., Sivanathan, A., Bosché, F., & Abdel-Wahab, M. (2016). Musculoskeletal disorders in construction: A review and a novel system for activity tracking with body area network. *Applied Ergonomics*, *54*, 120–130. https://doi.org/10.1016/j.apergo.2015.11.020

Van Nieuwenhuyse, A. (2006). The role of physical workload and pain related fear in the

development of low back pain in young workers: evidence from the BelCoBack Study: Results after one year of follow up. *Occupational and Environmental Medicine*, *63*(1), 45–52. https://doi.org/10.1136/oem.2004.015693

Winkel, J., & Mathiassen, S. E. (1994). Assessment of physical work load in epidemiologic studies: concepts, issues and operational considerations. *Ergonomics*, *37*(6), 979–988. https://doi.org/10.1080/00140139408963711

Yan, X., Li, H., Li, A. R., & Zhang, H. (2017). Wearable IMU-based real-time motion warning system for construction workers' musculoskeletal disorders prevention. *Automation in Construction*, *74*(Supplement C), 2–11. https://doi.org/10.1016/j.autcon.2016.11.007

Yan, X., Li, H., Wang, C., Seo, J., Zhang, H., & Wang, H. (2017). Development of ergonomic posture recognition technique based on 2D ordinary camera for construction hazard prevention through view-invariant features in 2D skeleton motion. *Advanced Engineering Informatics*, *34*, 152–163. https://doi.org/10.1016/j.aei.2017.11.001

Yost Labs. (2017). 3-Space™ Sensors. Retrieved April 19, 2018, https://yostlabs.com/3-space-sensors/

Yu, Y., Guo, H., Ding, Q., Li, H., & Skitmore, M. (2017). An experimental study of real-time identification of construction workers' unsafe behaviors. *Automation in Construction*, *82*, 193–206. https://doi.org/10.1016/j.autcon.2017.05.002

Yu, Y., Yang, X., Li, H., Luo, X., Guo, H., & Fang, Q. (n.d.). JVEC: a joint-level vision-based ergonomic assessment tool for construction workers. *Journal of Construction Engineering and Management*.

Zeng, W., Shu, L., Li, Q., Chen, S., Wang, F., & Tao, X.-M. (2014). Fiber-Based Wearable Electronics: A Review of Materials, Fabrication, Devices, and Applications. *Advanced Materials*, *26*(31), 5310–5336. https://doi.org/10.1002/adma.201400633

Zhou, X., Huang, Q., Sun, X., Xue, X., & Wei, Y. (2017). Towards 3D Human Pose Estimation in the Wild: a Weakly-supervised Approach. In *IEEE International Conference on Computer Vision*. http://arxiv.org/abs/1704.02447

Table 1. Joint capability regression coefficients

Joint	a	b	c	d
Right shoulder	0.17	16.26	0.17	23.35
Left shoulder	0.18	14.64	0.29	19.59
Right elbow	0.13	11.24	0.07	22.78
Left elbow	0.11	10.63	0.05	19.66
Right hip	0.33	19.19	0.66	34.44
Left hip	0.29	18.75	0.47	36.05
Right knee	0.16	8.78	0.08	22.47
Left knee	0.17	7.67	0.14	21.10

Table 2. Raw data

		Camera data		Insole plantar pressure data	
Activity	Duration [sec.]	Number of frames	Number of joints	Number of frames	Number of sensors
Material handling	22	550	16	1100	26
Plaster	19	475	16	950	26
Rebar	114	2853	16	5706	26
Total	155	3878	-	7756	-

Table 3. Values of all the right insole's 13 pressure sensors

Sensor Number	Pressure [N/cm^2]
0	1.25
1	1.50
2	1.00
3	0.50
4	1.00
5	3.00
6	0.25
7	5.25
8	2.50
9	5.75
10	5.5
11	4.24
12	5.25

Table 4. Examples joint torque calculation results

Joint torque	Joint capacity [N]	Frame#1 [N]	Frame#2 [N]	Frame#3 [N]
Right elbow	142.04	1.27	6.04	5.63
Right shoulder	107.24	4.52	4.34	5.29
Right knee	323.9	25.73	44.67	23.29
Right hip	276.37	51.58	85.89	27.41
Left elbow	125.97	1.89	4.88	3.57
Left shoulder	100.91	3.89	6.97	8.63
Left knee	313.54	35.1	64.86	103.69

Left hip	268.65	69.78	107.89	169.42

Table 5. Examples joint workload assessment results

Joint workload	Frame#1 [%]	Frame#2 [%]	Frame#3 [%]
Right elbow	1.27	6.04	5.63
Right shoulder	4.52	4.34	5.29
Right knee	25.73	44.67	23.29
Right hip	51.58	85.89	27.41
Left elbow	1.89	4.88	3.57
Left shoulder	3.89	6.97	8.63
Left knee	35.1	44.86	47.69
Left hip	49.78	47.89	49.42

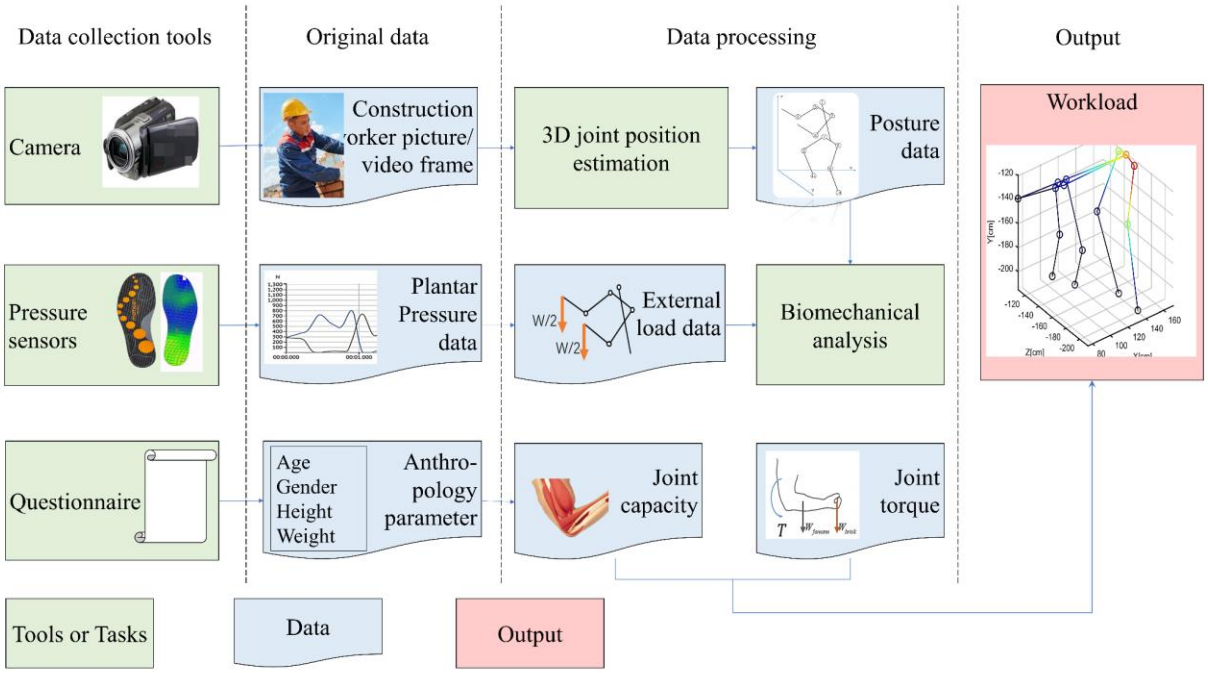

Figure 1 Outline of the automatic workload assessment method

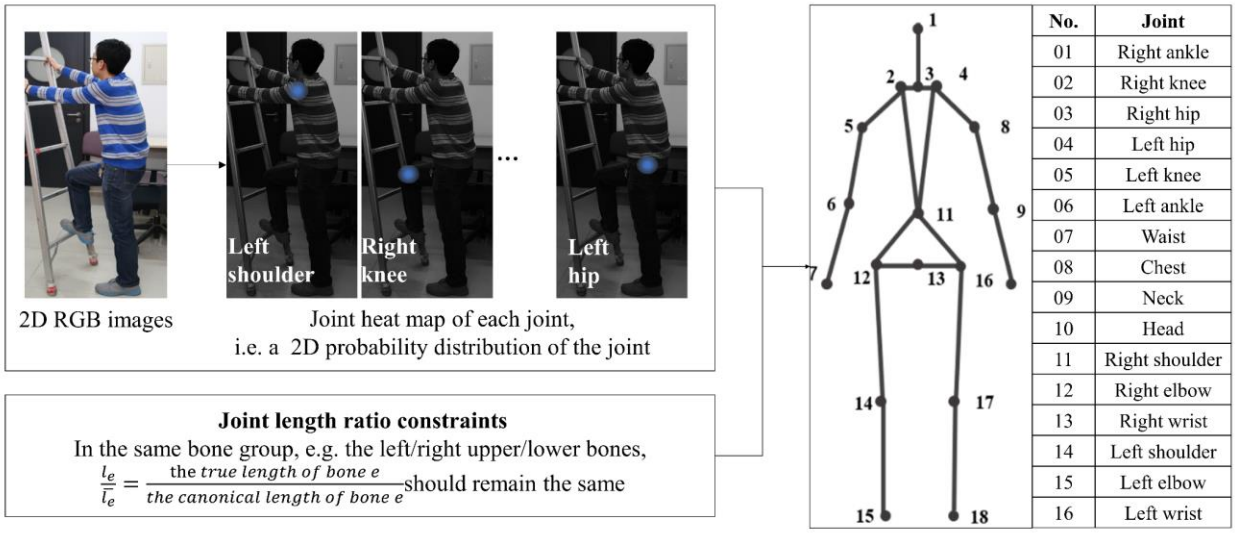

No.	Joint
01	Right ankle
02	Right knee
03	Right hip
04	Left hip
05	Left knee
06	Left ankle
07	Waist
08	Chest
09	Neck
10	Head
11	Right shoulder
12	Right elbow
13	Right wrist
14	Left shoulder
15	Left elbow
16	Left wrist

Figure 2 Framework of the 3D pose estimator

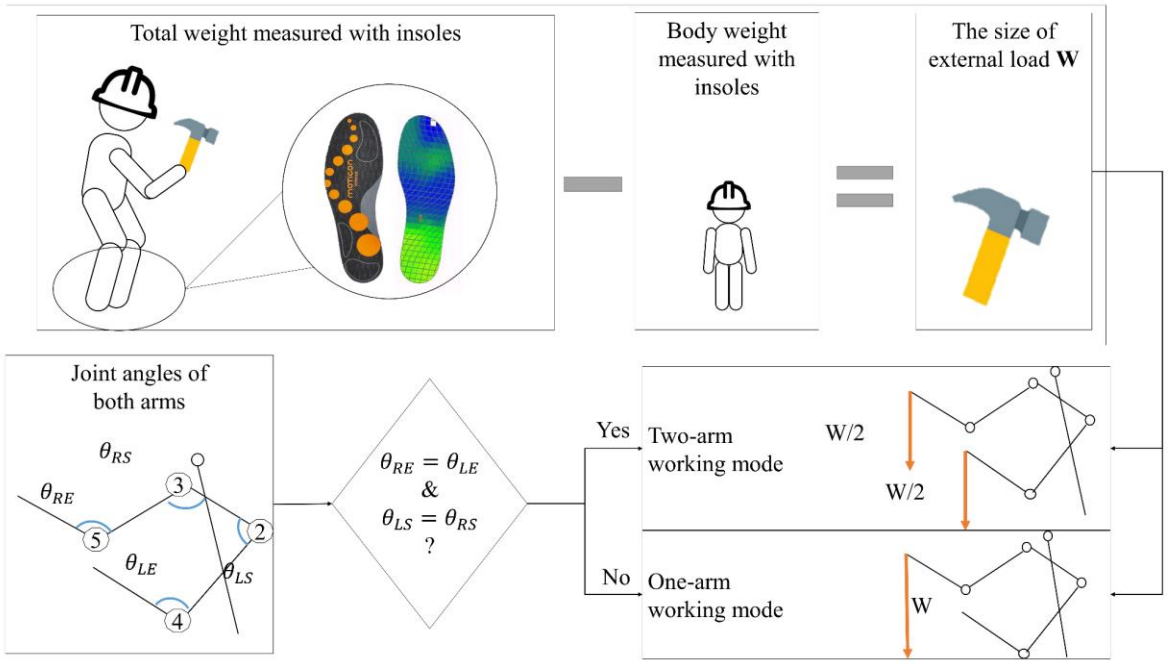

Figure 3 Calculation of external loads with smart insoles

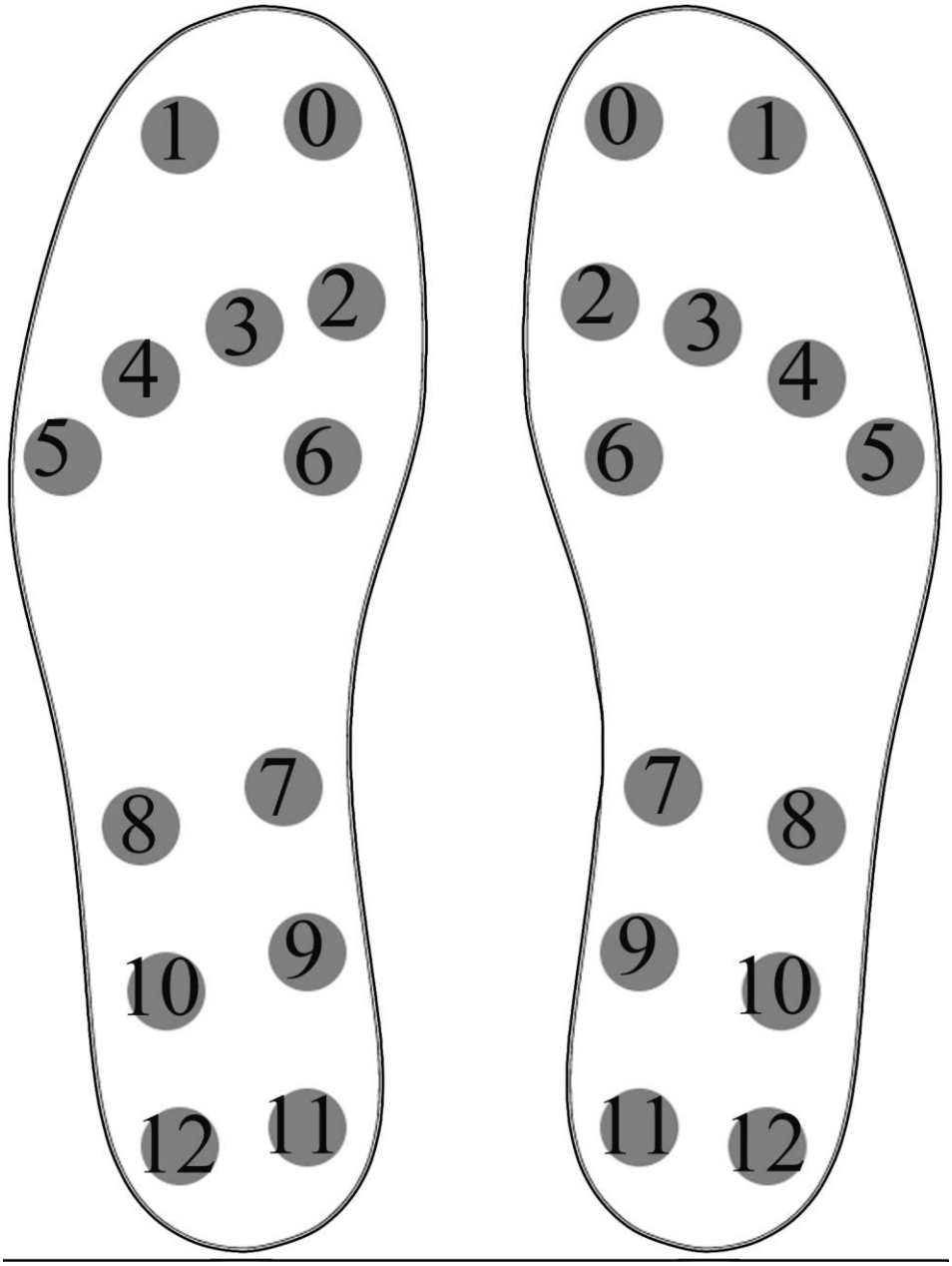

Figure 4 Distribution of sensors in a pair of smart insoles

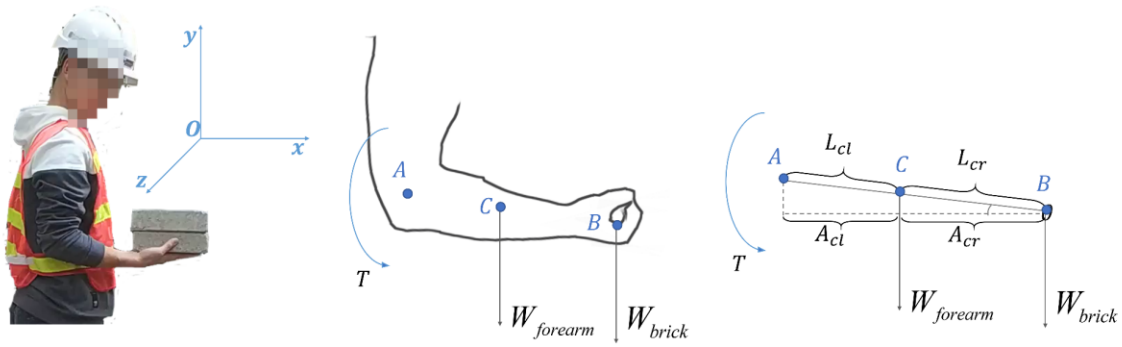

Figure 5 Biomechanical analysis of the elbow in equilibrium

Figure 6 Typical postures in material handling, rebar, and plastering

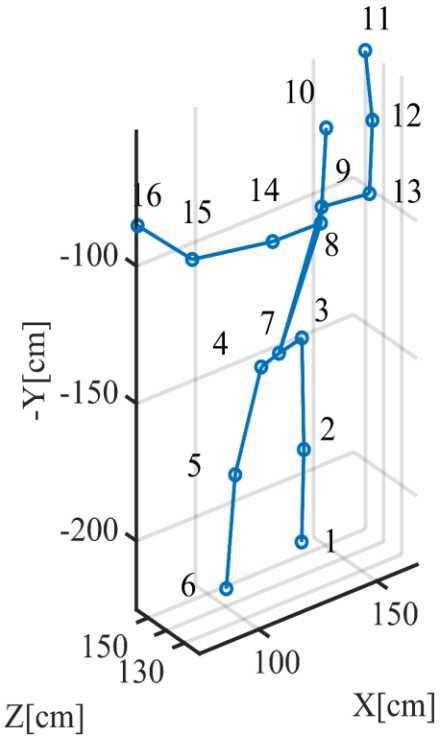

No.	Joint	X[cm]	Y[cm]	Z[cm]
01	Right ankle	145.00	225.00	156.52
02	Right knee	141.00	187.00	150.08
03	Right hip	139.00	145.00	148.55
04	Left hip	117.00	145.00	142.34
05	Left knee	113.00	187.00	151.53
06	Left ankle	107.00	225.00	148.58
07	Waist	127.00	145.00	145.52
08	Chest	127.00	87.00	122.39
09	Neck	127.00	81.00	122.01
10	Head	129.00	53.00	122.10
11	Right shoulder	167.00	51.00	150.11
12	Right elbow	159.00	67.00	135.70
13	Right wrist	147.00	83.00	121.68
14	Left shoulder	107.00	87.00	122.98
15	Left elbow	85.00	93.00	138.74
16	Left wrist	75.00	85.00	155.85

Figure 7 Example of 3D joint coordinate estimation during plastering

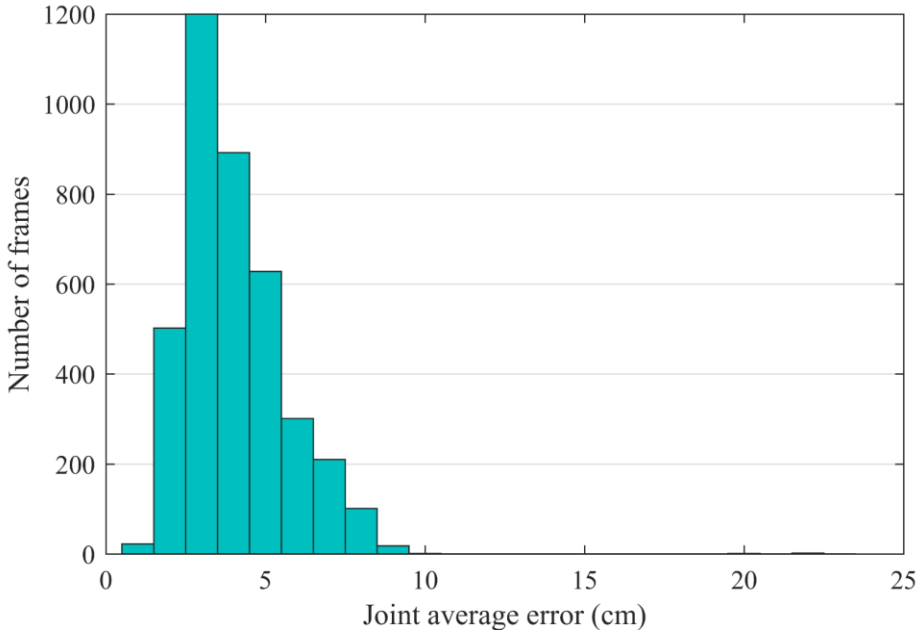

Figure 8 3D joint estimation error

Figure 9 Subject holding 0–4 bricks

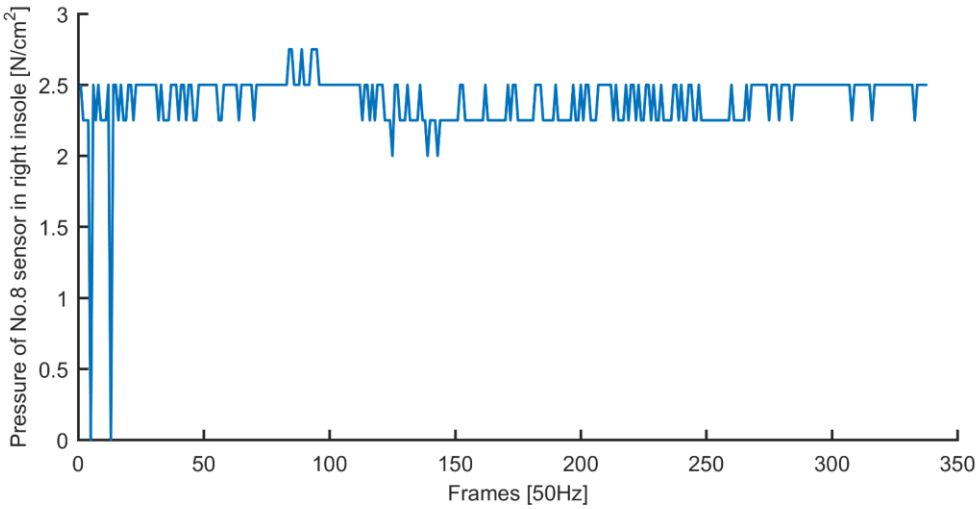

Figure 10 Pressure data of the No. 8 sensor in the right insole when the subject is carrying 3 bricks

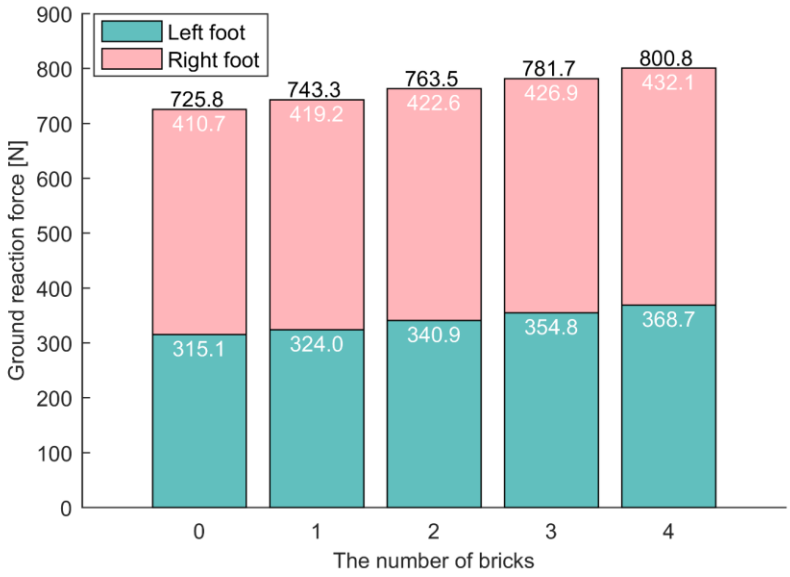

Figure 11 Ground reaction forces of both feet and total ground reaction forces when the subject is holding 0–4 bricks

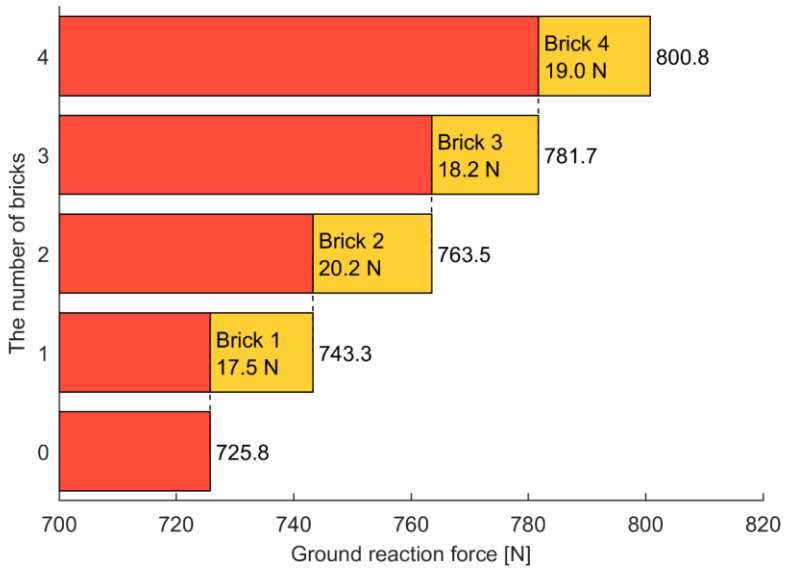

Figure 12 Calculating the weight of brick as the difference of total ground reaction forces

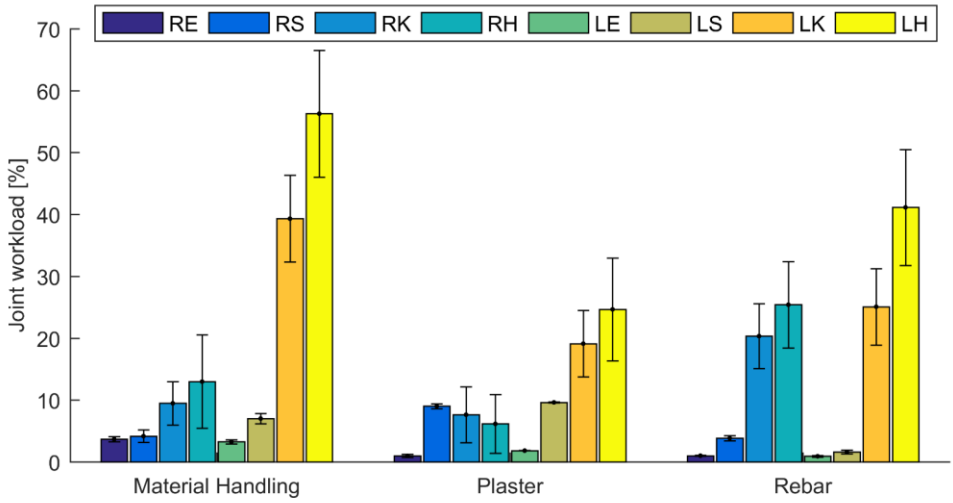

Figure 13 Calculating the weight of materials as the difference in total ground reaction force (L/R denotes left/right and E/S/K/H denotes elbow/shoulder/knee/hip.)

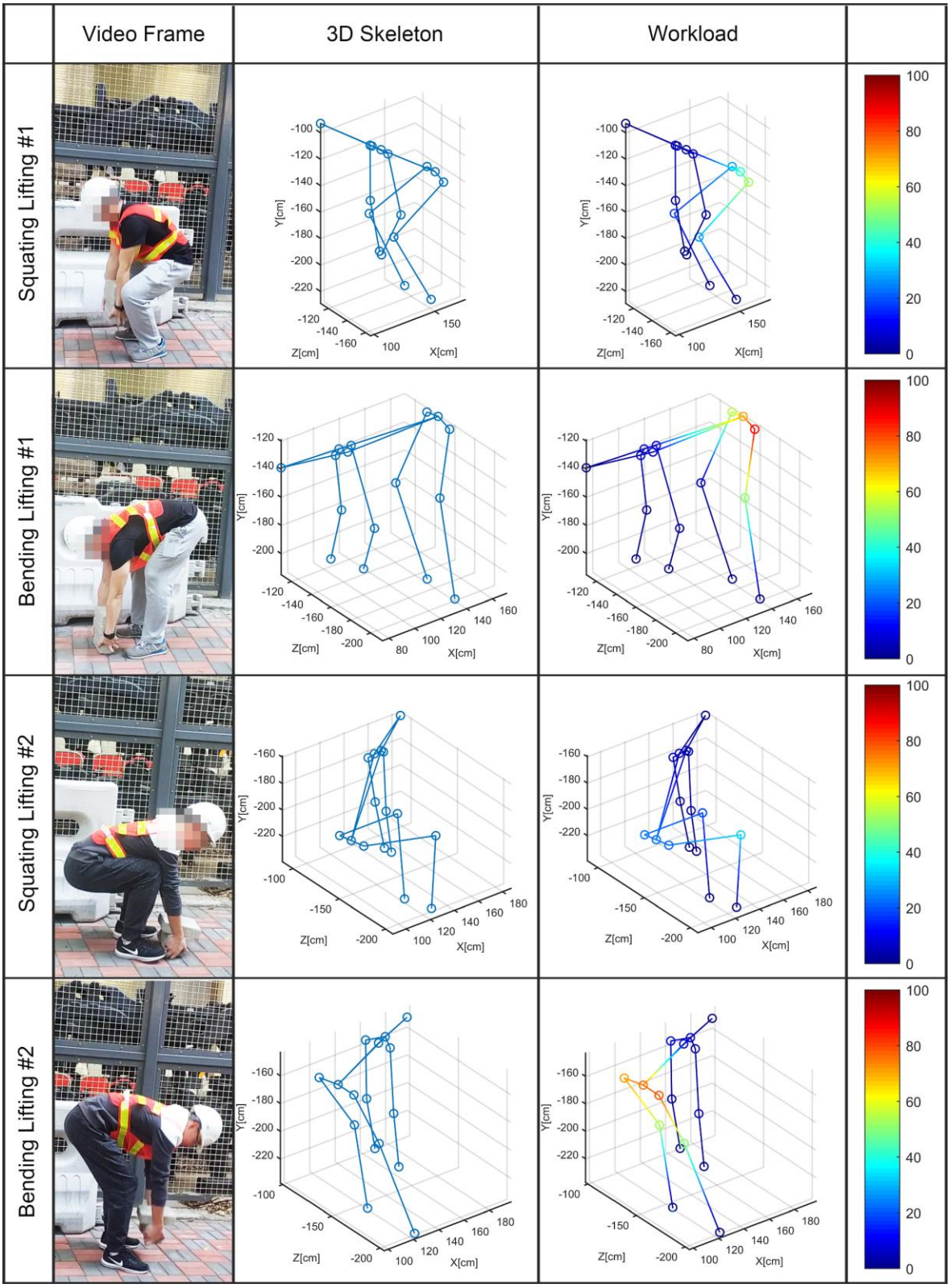

Figure 14 Visualizing the joint workload with the 3D skeleton

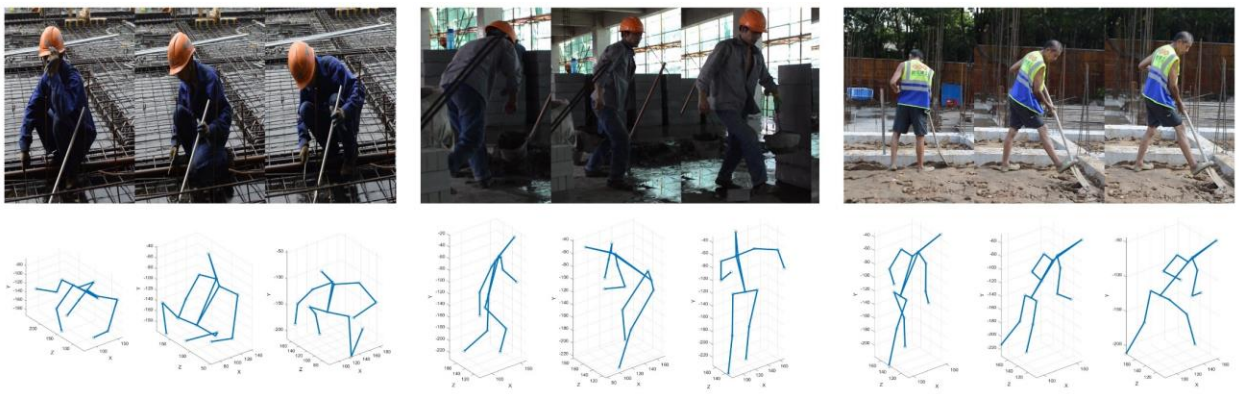

Figure 15 Example frames during the field test of the 3D motion capture method

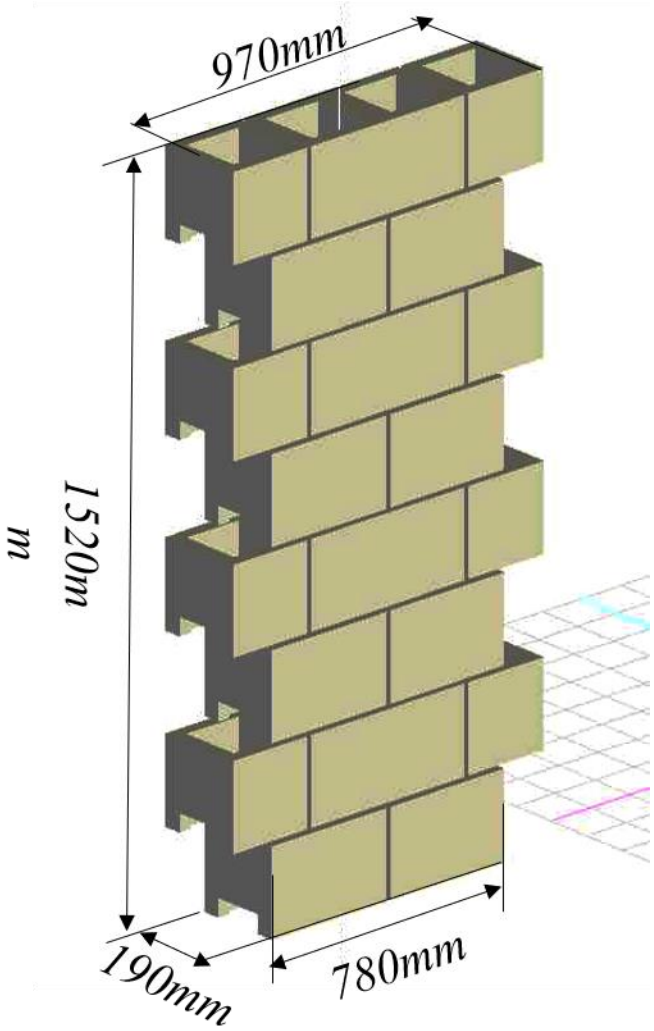

Figure 16 Design of the concrete block wall in the masonry task

Figure 17 One frame during the masonry task

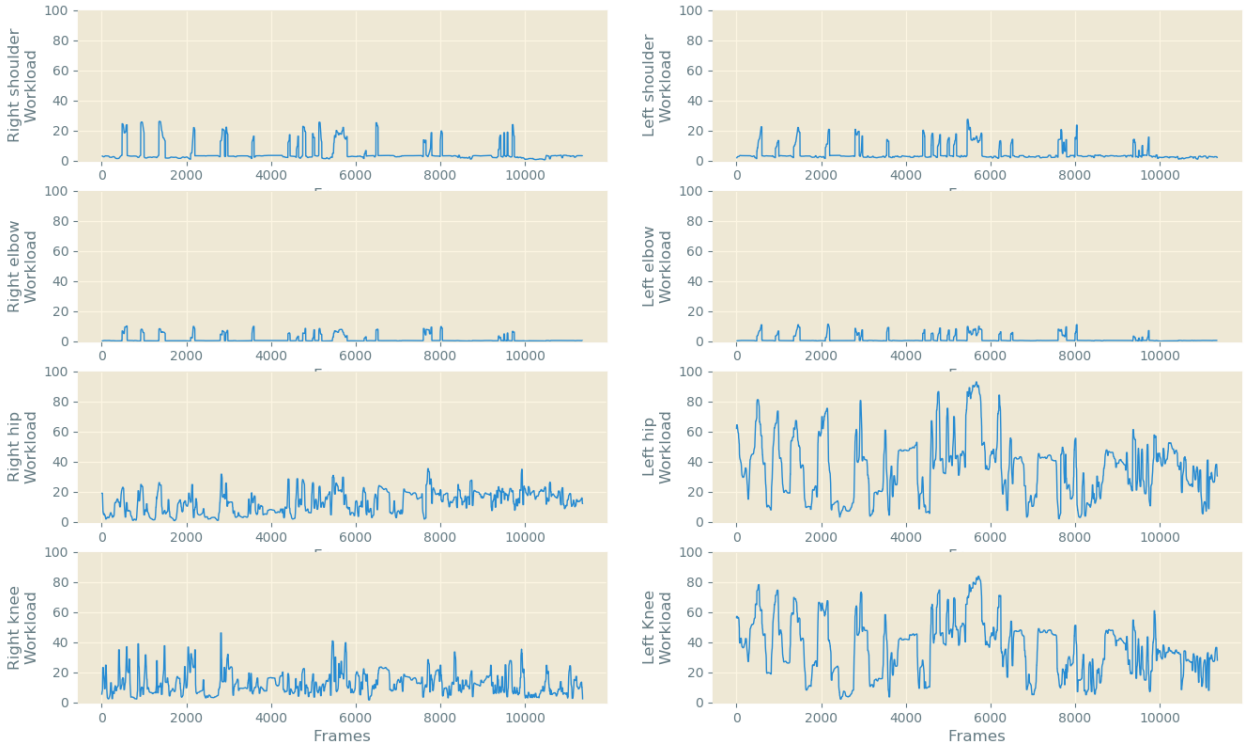

Figure 18 Joint-level workloads of each frame during the masonry task

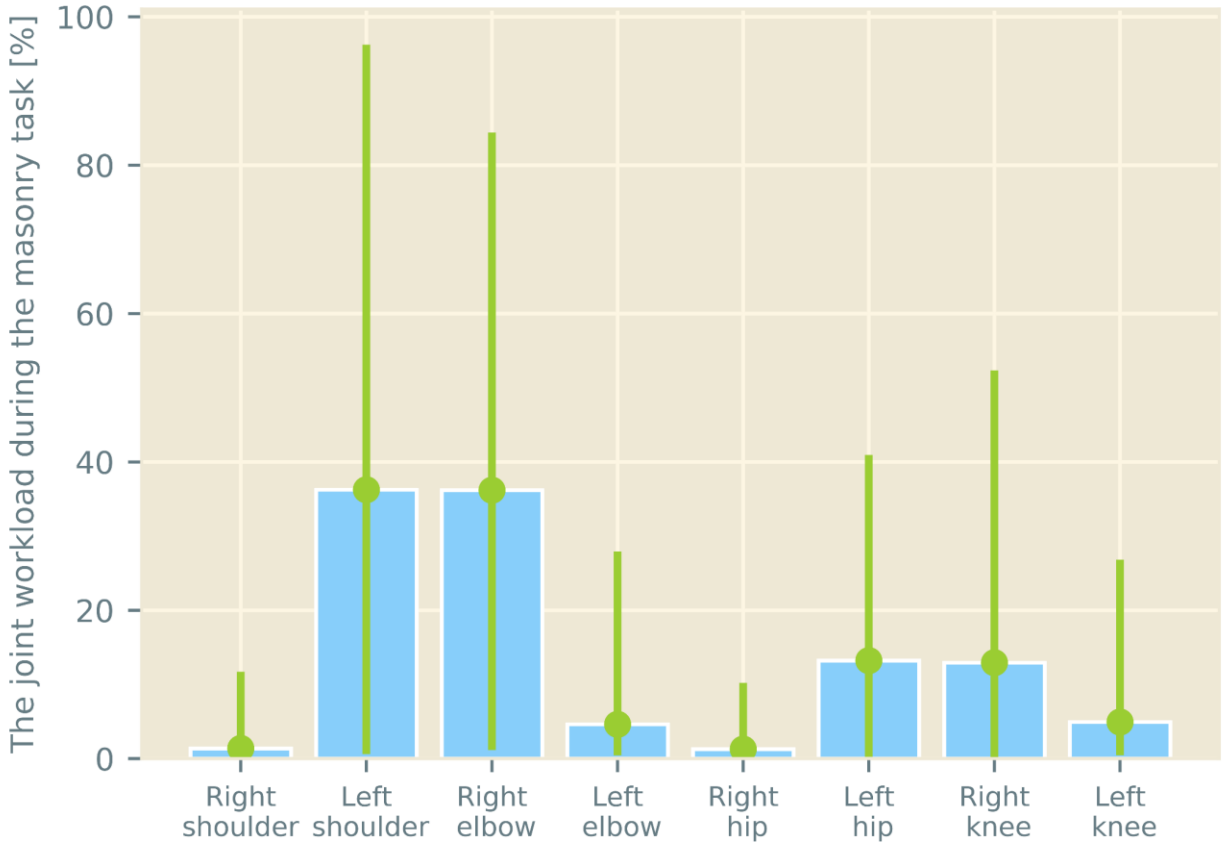

Figure 19 Average and range of the joint-level workloads during the masonry task